

# ON THE ORIGIN OF COSMIC-RAY IONISATION IN STAR-FORMING REGIONS

Marco Padovani<sup>1</sup>

**Abstract.** A field with particularly exciting results over the past few years is the study of the interaction of cosmic rays with interstellar matter. For star formation to take place, gas and dust need to be sufficiently cold for gravity to overcome thermal pressure, and the ionisation fraction must be low enough to enable substantial decoupling between the gas and the Galactic magnetic field. As soon as the visual extinction is of the order of 3 – 4 magnitudes, the ultraviolet photon flux from the interstellar radiation field is fully quenched, thus the only source of ionisation and heating is provided by low-energy cosmic rays. We will briefly focus on the Galactic and local origin of cosmic rays and on their effects on medium ionisation.

## 1 Tracing the presence of cosmic rays in star-forming regions

Cosmic rays (CRs) have a major impact on the chemical and dynamical evolution of star-forming regions. Their energy density ( $\sim 1 \text{ eV cm}^{-3}$ ) is of the order of that of the cosmic microwave background, the visible starlight, and the Galactic magnetic field (Ferrière, 2001). This makes CRs a major contributor to the energy budget of the interstellar medium.

Key questions such as (i) what are the mechanisms that determine the collapse of a molecular cloud, (ii) what are the basic processes that regulate the growth of dust grains, (iii) what is at the origin of the chemical complexity observed in clouds, and (iv) who is responsible for energetic phenomena such as the synchrotron emission observed at different scales of a cloud, find a common denominator in CRs (for a review, see Padovani et al., 2020). More precisely, it is the low-energy CRs ( $E < \text{TeV}$ ) that are relevant in answering the above questions, because the cross sections of the main processes occurring in molecular clouds (e.g., ionisation, dissociation, and excitation of  $\text{H}_2$  by CR protons and electrons) peak between about 10 eV and 10 keV (see, e.g. Padovani et al., 2009, 2018a). The core parameter that is employed in astrochemical codes to interpret the observed molecular abundances, as well as in non-ideal magnetohydrodynamic codes used to simulate, e.g., the collapse of a molecular cloud, is the so-called CR ionisation rate  $\zeta_{\text{H}_2}^{\text{ion}}$ . It represents the number of ionisations of hydrogen molecules by CRs per unit time and is defined by

$$\zeta_{\text{H}_2}^{\text{ion}} = 4\pi \int_I^{\infty} j(E)[1 + \Phi(E)]\sigma^{\text{ion}}(E) dE, \quad (0.1)$$

where  $I = 15.44 \text{ eV}$  is the  $\text{H}_2$  ionisation threshold,  $j(E)$  is the CR flux (or spectrum), namely the number of CRs per unit energy, time, area, and solid angle, the factor  $1 + \Phi(E)$  accounts for further ionisation by secondary electrons (see Ivlev et al., 2021), and  $\sigma^{\text{ion}}(E)$  is the ionisation cross section.

Over time, numerous techniques have been developed to estimate  $\zeta_{\text{H}_2}^{\text{ion}}$  through observations of molecular tracers. Depending on the region of the molecular cloud being observed, different tracers are used. In diffuse regions of molecular clouds, one of the most reliable, due to its simple network of formation and destruction reactions, is  $\text{H}_3^+$  (Oka, 2006), followed by  $\text{OH}^+$ ,  $\text{H}_2\text{O}^+$  (Neufeld et al., 2010), and  $\text{ArH}^+$  (Neufeld & Wolfire, 2017). In denser regions, other tracers are used, such as  $\text{HCO}^+$ ,  $\text{DCO}^+$ , and  $\text{CO}$  in low-mass dense cores (Caselli et al., 1998; Redaelli et al., 2021),  $\text{HCO}^+$ ,  $\text{N}_2\text{H}^+$ ,  $\text{HC}_3\text{N}$ ,  $\text{HC}_5\text{N}$ , and  $c\text{-C}_3\text{H}_2$  in protostellar clusters (Ceccarelli et al., 2014; Fontani et al., 2017; Favre et al., 2018), and, more recently,  $\text{H}_2\text{D}^+$  and other  $\text{H}_3^+$  isotopologues in high-mass star-forming regions (Bovino et al., 2020; Sabatini et al., 2020),  $\text{PO}^+$  towards the Galactic centre (Rivilla et al., 2022), and  $\text{H}_3\text{O}^+$ ,  $\text{SO}$ , and  $\text{HCN}$  isomers in the central molecular zone of the near starburst galaxy NGC 253 (Holdship et al., 2022; Behrens et al., 2022).

<sup>1</sup> INAF-Osservatorio Astrofisico di Arcetri, Largo E. Fermi 5, 50125 Firenze, Italy  
e-mail: marco.padovani@inaf.it

Each of these methods involves a different degree of uncertainty, which affects the degree of accuracy in determining the ionisation rate. For example,  $\text{H}_3^+$  observations can be carried out only towards specific lines of sight in the direction of early-type background stars. Moreover,  $\zeta_{\text{H}_2}^{\text{ion}}$  obtained through  $\text{H}_3^+$  is proportional to the gas volume density, the local ionisation fraction, and the details of the interstellar ultraviolet field attenuation, all of which affects the resulting ionisation rate estimate. In denser regions, the main drawback is that chemistry is much more complex than in diffuse clouds. This requires up-to-date, extensive reaction networks, and the main uncertainties come from the destruction and formation rates of several species, which are not well known, as well as the unconstrained amount of carbon and oxygen depletion on dust grains. Recently, [Bialy \(2020\)](#) introduced a new method to estimate  $\zeta_{\text{H}_2}^{\text{ion}}$  from the observations of near-infrared rovibrational transitions of  $\text{H}_2$ , mainly excited by secondary CR electrons. This method, refined and extended by [Padovani et al. \(2022\)](#), has been tested by [Bialy et al. \(2022\)](#), obtaining upper limits of  $\zeta_{\text{H}_2}^{\text{ion}}$ . In principle, the James Webb Space Telescope should be able to detect these near-infrared  $\text{H}_2$  lines, making it possible to derive, for the first time, spatial variation of  $\zeta_{\text{H}_2}^{\text{ion}}$  in dense gas and to test competing models of CR propagation and attenuation in the interstellar medium ([Everett & Zweibel, 2011](#); [Morlino & Gabici, 2015](#); [Silsbee & Ivlev, 2019](#); [Padovani et al., 2018b](#); [Gaches et al., 2021](#)).

## 2 Galactic or local cosmic rays?

Figure 0.1 shows the most up-to-date collection of observational estimates of  $\zeta_{\text{H}_2}^{\text{ion}}$  as a function of  $\text{H}_2$  column density. The black solid lines show the trends predicted by theoretical models ([Padovani et al., 2018b, 2022](#)). The model  $\mathcal{L}$ , based on Voyager data ([Cummings et al., 2016](#); [Stone et al., 2019](#)), clearly underestimates the ionisation rate in diffuse clouds ( $N_{\text{H}_2} \lesssim 10^{21} \text{ cm}^{-2}$ ). Even though the Voyager probes have in all probability passed the heliopause, they are far from measuring the intensity of the average Galactic CR flux. Therefore, theoretical models empirically assume the existence of a higher CR flux below about 650 MeV, decreasing the spectral slope,  $\alpha$ , from 0.1 (Voyager-like spectrum) to  $-0.8$  (model  $\mathcal{H}$ ) to  $-1.2$ . The models thus succeed in providing an envelope of expected values for  $\zeta_{\text{H}_2}^{\text{ion}}$  assuming that the origin of CRs propagating in molecular clouds is Galactic. We note that estimates of  $\zeta_{\text{H}_2}^{\text{ion}}$  under the model  $\mathcal{L}$  could be due to uncertainties in the chemical model.

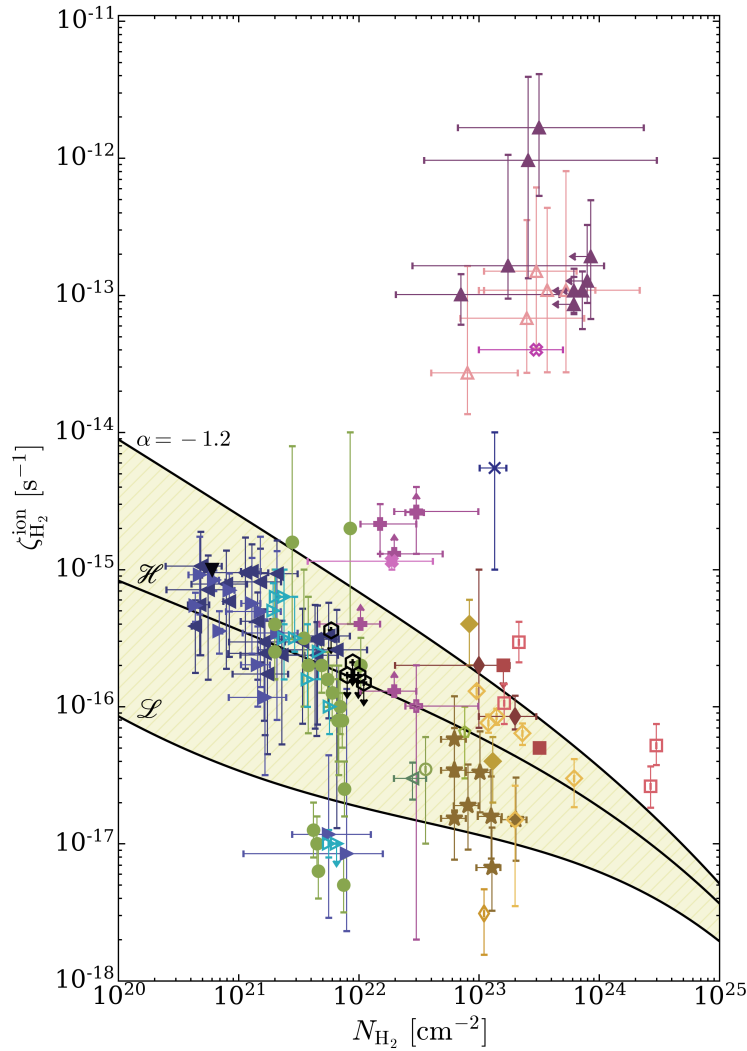
The apparent decrease of  $\zeta_{\text{H}_2}^{\text{ion}}$  with increasing  $N_{\text{H}_2}$  is confirmed by the kernel density estimation (KDE) shown in Fig. 0.2. The latter was obtained by considering only  $\zeta_{\text{H}_2}^{\text{ion}}$  estimates compatible with the average Galactic CR spectrum, associating a 30% error with the measurements where the error was not estimated, and removing all upper limits. The KDE contains a sort of bias as most  $\zeta_{\text{H}_2}^{\text{ion}}$  estimates are at  $N_{\text{H}_2} \lesssim 10^{22} \text{ cm}^{-2}$  and around  $10^{23} \text{ cm}^{-2}$ , yet the trend is reasonably evident. This confirms what is predicted by the theoretical models, namely that the flux of CRs (and therefore their ionising power) is attenuated as they propagate in molecular clouds losing energy through collisions with ambient  $\text{H}_2$ .

Figure 0.1 shows a large number of  $\zeta_{\text{H}_2}^{\text{ion}}$  that cannot be explained by the average Galactic CR flux. These values were measured in molecular clouds near supernova remnants, in protostellar clusters, towards the Galactic centre, and in the central zone of an external galaxy. These recent measurements provide increasingly clear evidence of the presence of locally produced CRs within the sources themselves. The first models introduced by [Padovani et al. \(2015, 2016\)](#) explain the local production of CRs through the acceleration of thermal particles at the shock surfaces (along the protostellar jets and on the protostellar surfaces), according to the first-order Fermi acceleration mechanism (e.g. [Drury et al., 1996](#)). The maximum energies reached by these CRs are of the order of 0.1 – 10 GeV, that is much lower than those expected in supernova remnant shocks. However, their flux is sufficient to explain the observations of these extreme  $\zeta_{\text{H}_2}^{\text{ion}}$  as well as the synchrotron emission detected in protostellar jets (e.g. [Sanna et al., 2019](#)) and H II regions (e.g. [Meng et al., 2019](#)). In addition, an important by-product of local acceleration models is the possibility of constraining physical quantities such as magnetic field strength, volume density, and flow velocity in the shock reference frame ([Padovani et al., 2019, 2021](#)).

## 3 Local cosmic-ray sources: a new line of research

In recent years, the theory of local production of CRs within molecular clouds has opened up a new area of investigation. Several research groups are developing theories and observational applications on the effects of these local CRs from M-dwarfs on Earth-like exoplanetary atmospheres (e.g. [Tabataba-Vakili et al., 2016](#)), their propagation in T Tauri winds (e.g. [Fraschetti et al., 2018](#)), their effect on protoplanetary discs (e.g. [Rodgers-Lee et al., 2017](#)), and their impact in protostellar clusters (e.g. [Gaches & Offner, 2018](#); [Gaches et](#)

al., 2019). Research in this new domain will be supported by current and next generation telescopes, such as: SKA and its precursors (e.g. MeerKAT, LOFAR), for synchrotron emission at different scales; CTA, for  $\gamma$ -ray emission from high-mass protostars and H II regions; and ELT/HIRES, JWST, and ARIEL, for the impact of CRs on habitability and exoplanetary atmospheres.



**Figure 0.1.** Total CR ionisation rate as a function of the  $\text{H}_2$  column density: theoretical model  $\mathcal{L}$ ,  $\mathcal{H}$  and with low-energy spectral slope  $\alpha = -1.2$  (solid black lines) from Padovani et al. (2022). The hatched-filled region show the expected  $\zeta_{\text{H}_2}^{\text{ion}}$  range in case where ionisation is due to the average Galactic CR flux. Observational estimates: in diffuse clouds by Shaw et al. (2008, solid downward-pointing triangle), Indriolo & McCall (2012, solid left-pointing triangles), Neufeld & Wolfire (2017, solid right-pointing triangles), Luo et al. (2023, empty right-pointing triangles); in low-mass dense cores by Caselli et al. (1998, solid circles), Maret & Bergin (2007, empty circle), Fuente et al. (2016, empty pentagon), Redaelli et al. (2021, empty left-pointing triangle) Bialy et al. (2022, empty hexagons); in high-mass star-forming regions by Sabatini et al. (2020, stars), de Boisanger et al. (1996, solid diamonds), van der Tak et al. (2000, empty diamonds), Hezareh et al. (2008, empty thin diamonds), Morales Ortiz et al. (2014, solid thin diamonds); in circumstellar discs by Ceccarelli et al. (2004, solid squares); in massive hot cores by Barger & Garrod (2020, empty squares); in molecular clouds close to supernova remnants by Ceccarelli et al. (2011, solid cross), Vaupré et al. (2014, solid plus signs); in a protostellar cluster by Ceccarelli et al. (2014, empty cross); towards the Galactic centre by Rivilla et al. (2022,  $\times$  sign); towards the central molecular zone of NGC 253 by Holdship et al. (2022, empty up-pointing triangles) and Behrens et al. (2022, solid up-pointing triangles).

## References

- Barger, C. J., & Garrod, R. T. 2020, *ApJ*, 888, 38
- Behrens, E., Mangum, J. G., Holdship, J. 2022, *ApJ*, 939, 119
- Bialy, S. 2020, *Commun. Phys.*, 3, 32
- Bialy, S., Belli, S., & Padovani, M. 2022, *A&A*, 658, L13

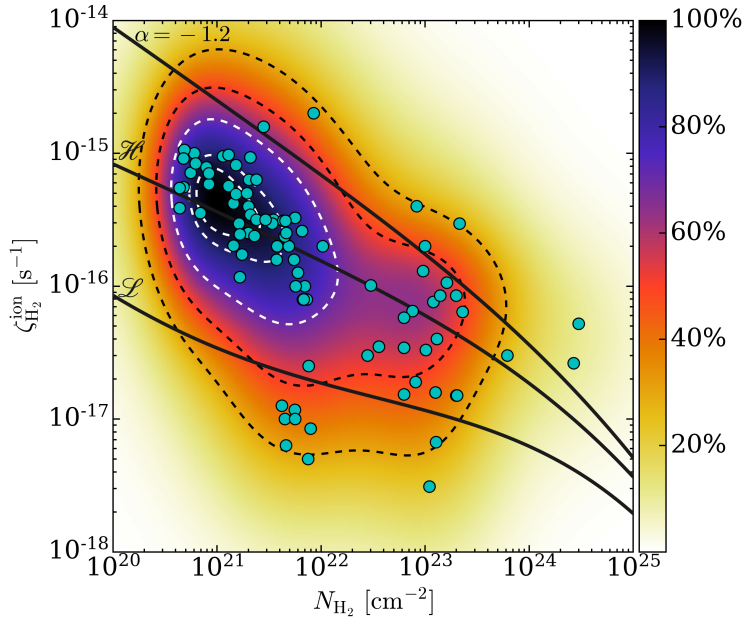


**Figure 0.2.** Kernel density estimation (KDE) of the CR ionisation rate (colour map) by considering only sources ionised by Galactic CRs (see Fig. 0.1 for references to models and observations). Dashed contours show 30, 50, 70, 90, and 95% of the KDE. Solid black lines represent the theoretical models from Padovani et al. (2022).

- Bovino, S., Ferrada-Chamorro, S., Lupi, A. et al. 2020, MNRAS 495, L7
- Caselli, P., Walmsley, C. M., Terzieva, R. et al. 1998, ApJ, 499, 234
- Ceccarelli, C., Dominik, C., Lefloch, B. et al. 2004, ApJ, 607, L51
- Ceccarelli, C., Hily-Blant, P., Montmerle, T. et al. 2011, ApJ, 740, L4
- Ceccarelli, C., Dominik, C., López-Sepulcre, A., et al. 2014, ApJ, 790, L1
- Cummings, A. C., Stone, E. C., Heikkila, B. C., et al. 2016, ApJ, 831, 18
- de Boisanger, C., Helmich, F. P., & van Dishoeck, E. F. 1996, A&A, 310, 315
- Drury, L. O’C., Duffy, P., & Kirk, J. G. 1996, A&A, 309, 1002
- Everett, J. E., & Zweibel, E. G. 2011, ApJ, 739, 60
- Favre, C., Ceccarelli, C., López-Sepulcre, A., et al. 2018, ApJ, 859, 136
- Ferrière, K. M. 2001, Rev. Mod. Phys., 73, 1031
- Fontani, F., Ceccarelli, C., Favre, C., et al. 2017, A&A, 605, A57
- Fraschetti, F., Drake, J. J., Cohen, O., et al. 2018, ApJ, 853, 112
- Fuente, A., Cernicharo, J., Roueff, E., et al. 2016, A&A, 593, A94
- Gaches, B. A. L. & Offner, S. S. R., 2018, ApJ, 861, 87
- Gaches, B. A. L., Offner, S. S. R., & Bisbas, T. G. 2019, ApJ, 878, 105
- Gaches, B. A. L., Walch, S., & Lazarian, A. 2021, ApJ, 917, L39
- Hezareh, T., Houde, M., McCoey, C., et al. 2008, ApJ, 684, 1221
- Holdship, J., Mangum, J. G., Viti, S. et al. 2022, ApJ, 931, 89
- Indriolo, N., & McCall, B. J. 2012, ApJ, 745, 91
- Ivlev, A. V., Silsbee, K., Padovani, M. et al. 2021, ApJ, 909, 107
- Luo, G., Zhang, Z.-Y., Bisbas, T. G., et al. 2023, ApJ, 942, 101

- Maret, S., & Bergin, E. A. 2007, *ApJ*, 664, 956
- Padovani, M., Marcowith, A., Sánchez-Monge, Á., et al. 2019, *A&A*, 630, A72
- Morales Ortiz, J. L., Ceccarelli, C., Lis, D. C., et al. 2014, *A&A*, 563, A127
- Morlino, G., & Gabici, S. 2015, *MNRAS*, 451, L100
- Neufeld, D. A., Goicoechea, J. R., Sonnentrucker, P., et al. 2010, *A&A*, 521, L10
- Neufeld, D. A., & Wolfire, M. G. 2017, *ApJ*, 845, 163
- Oka, T. 2006, *Proc. Natl. Acad. Sci.*, 103, 12235
- Padovani, M., Galli, D., & Glassgold, A. E. 2009, *A&A*, 501, 619
- Padovani, M., Hennebelle, P., Marcowith, A., et al. 2015, *A&A*, 582, L13
- Padovani, M., Marcowith, A., Hennebelle, P., et al. 2016, *A&A*, 590, A8
- Padovani, M., Galli, D., Ivlev, A. V., et al. 2018a, *A&A*, 619, A144
- Padovani, M., Ivlev, A. V., Galli, D. et al. 2018b, *A&A*, 614, A111
- Padovani, M., Marcowith, A., Sánchez-Monge, Á, et al. 2019, *A&A*, 630, A72
- Padovani, M., Ivlev, A. V., Galli, D., et al. 2020, *Space Sci. Rev.*, 216, 29
- Padovani, M., Marcowith, A., Galli, D., et al. 2021, *A&A*, 649, A149
- Padovani, M., Bialy, S., Galli, D., et al. 2022, *A&A*, 658, A189
- Redaelli, E., Sipilä, O., Padovani, M., et al. 2021, *A&A* 656, A109
- Rivilla, V. M., de la Concepción, J. G., Jiménez-Serra, I. et al. 2022, *FrASS*, 9, 829288
- Rodgers-Lee, D., Taylor, A. M., Ray, T.P., et al. 2017, *MNRAS*, 472, 26
- Sabatini, G., Bovino, S., Giannetti, A., et al. 2020, *A&A*, 644, A34
- Sanna, A., Moscadelli, L., Goddi, C., et al., 2019, *A&A*, 623, L3
- Shaw, G., Ferland, G. J., Srianand, R., et al. 2008, *ApJ*, 675, 405
- Silsbee, K., & Ivlev, A. V. 2019, *ApJ*, 879, 14
- Stone, E. C., Cummings, A. C., Heikkila, B. C., et al. 2019, *Nat. Astron.*, 3, 1013
- Tabataba-Vakili, F., Grenfell, J. L., Griebmeier, J. M., et al. 2016, *A&A*, 585, A96
- van der Tak, F. F. S., van Dishoeck, E. F., Evans, Neal J., I., et al. 2000, *ApJ*, 537, 283
- Vaupré, S., Hily-Blant, P., Ceccarelli, C. et al. 2014, *A&A*, 568, A50